Shared potential metabolism trends in degraded soils and type 2 diabetes gut microbiomes

Craig Liddicoat[1,*], Bart A. Eijkelkamp[1], Timothy R. Cavagnaro[1], Jake M. Robinson[1], Kiri Joy Wallace[2], Andrew D. Barnes[2], Garth Harmsworth[3], Damien J. Keating[4], Robert A. Edwards[1] and Martin F. Breed[1]

[1]College of Science and Engineering, Flinders University, Bedford Park, South Australia, Australia
[2]Te Aka Mātuatua – School of Science, University of Waikato, Hamilton, Aotearoa New Zealand
[3]Manaaki Whenua – Landcare Research, Palmerston North, Aotearoa New Zealand
[4]College of Medicine and Public Health, Flinders University, Bedford Park, South Australia, Australia

***Corresponding author:** Craig Liddicoat; craig.liddicoat@flinders.edu.au

ORCIDs: CL: 0000-0002-4812-7524, BAE: 0000-0003-0179-8977, TRC: 0000-0002-9922-5677, JMR: 0000-0001-8108-3271; KJW: 0000-0003-1236-6846, ADB: 0000-0002-6499-381X, GH: 0000-0002-7041-1847, DJK: 0000-0002-0154-8305, RAE: 0000-0001-8383-8949, MFB: 0000-0001-7810-9696

Competing Interest Statement: The authors declare no competing interest.

Keywords: Healthy microbiome, type 2 diabetes, metagenomics, compound processing potential, soil biodiversity, human health, metabolism, branched-chain fatty acids

Abstract

Microbiome-mediated impacts of global change on human metabolic health remain understudied. Type 2 diabetes (T2D) is shaped by nutrition, host and environmental factors, with rapidly increasing global prevalence. Soil microbiomes shift with ecosystem degradation and may influence human metabolism through altering food quality and gut microbiomes, including metabolite exposures without requiring colonization. Here, we investigated functional overlaps between soil microbiomes across ecosystem degradation gradients (USA, Australia) and gut microbiomes in T2D versus normal health (Sweden, China). We developed a method to translate metagenomic functional pathways to potential metabolism of biochemical compounds. In silico trend analyses revealed consistent shifts relevant to energy harvesting and management. Both T2D gut microbiomes and degraded soil microbiomes exhibited increased potential metabolism for sugars and decreased potential metabolism for lignin and monomethyl branched-chain fatty acids. Our findings suggest ecosystem degradation may contribute to T2D pathogenesis through nutrient-depleted food and/or adverse shaping of gut microbiome functional capacities.

41 **Introduction**

42 Microbiomes connect ecosystems and humans under One Health[1, 2]. Yet, microbiome-mediated impacts
43 of accelerating global change[3] on human metabolic health have received little attention. Type 2
44 diabetes (T2D) is a major chronic multifaceted metabolic disease, characterized by insulin resistance
45 and high blood sugar, and linked to host, nutritional and environmental factors[4, 5, 6]. As the health and
46 economic burden of T2D rise rapidly worldwide[7, 8], understanding its complex pathogenesis is critical.
47 The human gut microbiome is integral to our metabolism[9, 10] with a vast enzymatic repertoire that
48 complements human digestive capabilities[11] and produces metabolites that modulate appetite, gut
49 motility, hormonal signaling and gene expression[10]. Gut microbiomes shift in T2D and with metformin
50 treatment[12], while fecal microbiome transplantations can improve clinical outcomes[13, 14]. Given that
51 long-term diet and environmental exposures have major influences on the gut microbiome[15, 16], which
52 is intricately linked to metabolism and T2D risk, there is a pressing need to identify upstream
53 nutritional and environmental factors that influence this crucial interface to human metabolic health.

54 Beyond diet and lifestyle factors, environmental exposures are increasingly recognized as
55 contributors to T2D risk[5], including shifts from rural to urban areas[17, 18, 19, 20]. Microbiomes are a
56 hypothesized link between environments and gut-associated health[21, 22]. Soils are the dominant
57 reservoir of microbial life[23, 24], and exposure to diverse soil microbiomes (for example, via direct
58 contact, food and airborne dust), especially from a young age, can shape gut microbiomes[16, 21, 25, 26, 27].
59 In wild primates, gut communities vary with environmental heterogeneity, especially soil differences[28].
60 Soil microbiomes also shape food quality by driving nutrient cycling and gathering[29], incorporating
61 microbial metabolites into plants[30], and influencing gut microbiota of ruminants[31]. Beyond the
62 microbes per se, microbiomes also comprise important metabolites (for example, biochemical
63 compounds, constituent molecules) and potentially transferable genetic material[32] with diverse
64 structural, functional and nutritional roles[9, 30, 33]. In soils and the gut, a vast range of metabolites with

65 varying bioactivities may be accumulated, depleted and/or transferred via microbial activity and
66 turnover[9, 34]. This means microbiomes can extend their influence via metabolites and necromass
67 without requiring direct colonization. While the survival of soil microbes in the gut may be low or
68 uncertain, the shaping of gut microbiomes by soil microbiome exposures is well-recognized[1, 35].
69 Moreover, soil microbiome composition and functional capacities may shift in generalizable ways with
70 ecosystem degradation, for example, via urbanization and land-use change, with potential to impact
71 human health[36, 37, 38, 39]. Together, these phenomena create pathways whereby degraded environments
72 may adversely shape soil microbiomes, food quality and gut microbiomes, and potentially contribute to
73 metabolic dysfunction in T2D.

74 In ongoing work to define 'healthy microbiomes', approaches based on community-scale
75 functional capacity (rather than taxonomy) should provide greater insight[40, 41]. Notably, many processes
76 involve assemblages using shared resources in extracellular space[9]. Striving for deeper functional
77 insights and interpretability, metabolite- or compound-oriented approaches[38] aim to move beyond
78 metabolic pathways towards measures related to specific chemical compounds (such as carbohydrates,
79 lipids, proteins, often linked to microbial feedstocks or by-products; Supplementary Fig. 1).
80 Compound-scale insights should offer more foundational information (as compounds can underpin
81 multiple functional pathways), benefit from known links to biochemistry and host health, and may
82 point to new mechanistic hypotheses and therapeutic targets. However, existing metabolite prediction
83 frameworks[42, 43, 44] rely on organism-specific and environment-specific approaches unsuited to highly
84 biodiverse, poorly characterized and varying environments, such as soils[38]. Therefore, there is a need
85 for new, compound-oriented methods to examine normal versus aberrant functioning in comparative
86 analyses across soil and gut microbiomes.

87 In this integrative in silico study, we explored potential links between ecosystem degradation
88 and metabolic alterations in the T2D gut by examining functional overlaps between soil microbiomes

89 across ecosystem degradation gradients and gut microbiomes in T2D versus normal health (datasets are
90 described in Supplementary Table 1). We translated metagenomic functional gene-associated
91 biochemical pathways to 'compound processing potential' (CPP, %), reflecting potential metabolism of
92 individual compounds. While not measuring compounds directly, our method quantified the capacity of
93 metagenomes to metabolize (or process) them. Reactants and products were not differentiated, as
94 compounds can be inputs and outputs of various processes. Examining (1) 30 selected compounds
95 relevant to soil and gut health (Supplementary Table 2) and (2) via exhaustive compound-wide trend
96 analyses, we identified compounds relevant to energy harvesting and management that shared potential
97 metabolism (i.e., CPP) trends. In a staged approach, we first examined soils from a forest restoration
98 chronosequence[45] (from the United States, US; spanning degraded post-mining, reforested, and
99 unmined reference sites), then progressively considered overlapping CPP trends in T2D versus control
100 cohorts from Sweden[46] and then China[47]. Lastly, we sought corroboration of overlapping trends in a
101 'disturbed versus natural' soil dataset from the Australian Microbiome Initiative (AMI[48], described in
102 ref.[38]; see Supplementary Table 1).
103

104 ## Results

105 **Trends with ecosystem degradation**

106 For the 30 selected compounds we assessed trends with ecosystem degradation in the chronosequence
107 soils (US) (Supplementary Table 2; Supplementary Figs. 2-31) and found increased potential
108 metabolism for ($P < 0.001$) D-fructose, sucrose, L-arabinose, D-glucose, xylose and chitin; also ($P <$
109 0.01) galactose, mannose and hydrogen sulfide; and ($P \leq 0.05$) glucosamine and arabinoxylan
110 (hemicellulose). We found decreased potential metabolism with ecosystem degradation for ($P < 0.001$)
111 lignin, acetate and carbon dioxide; also ($P < 0.01$) glycogen, butyrate, trimethylamine N-oxide and
112 trimethylamine; and ($P \leq 0.05$) propionate and methane.

113 Compound-wide trend analyses identified 2,122 compounds with significant CPP trends (n =
114 757 decreased, n = 1,365 increased with ecosystem degradation; compound and trend data are in
115 Supplementary Material files). Carbon-containing compounds were mapped using chemical formula
116 ratios oxygen:carbon (O:C), hydrogen:carbon (H:C) and nitrogen:carbon (N:C) (Fig. 1) to visualize
117 energetically and chemically similar compounds that trend together (see example plot that visualizes all
118 carbon-containing compounds within a single sample in Supplementary Fig. 32).
119
120 **Trends in type 2 diabetes**
121 For the 30 selected compounds, we found consistent trends in the Swedish (SWE) and Chinese (CHN)
122 cohort datasets (Supplementary Table 2; Supplementary Figs. 2-31, 33) for increased potential
123 metabolism in T2D for D-fructose (SWE: $P \leq 0.05$, CHN: $P < 0.01$), L-arabinose (SWE: $P \leq 0.05$,
124 CHN: $P < 0.001$), and amylopectin (SWE and CHN: $P \leq 0.05$); and decreased potential metabolism in
125 T2D for lignin (SWE and CHN: $P \leq 0.05$).
126 Numerous trends were only found in one T2D cohort or the other. Increased potential
127 metabolism was found in T2D in the Swedish cohort for sucrose and starch ($P \leq 0.05$), and in the
128 Chinese cohort for mannose ($P < 0.001$); glucose, galactose and xylose (all $P < 0.01$). Decreased
129 potential metabolism was found in T2D in the Chinese cohort for acetate, propionate, butyrate, carbon
130 dioxide, hydrogen sulfide, indole (all $P < 0.001$); menaquinone (Vitamin K2), glucosamine ($P < 0.01$);
131 methane, p-cresol and serotonin (all $P \leq 0.05$). We found conflicting potential metabolism trends for
132 ammonia in T2D, which increased in Swedish ($P < 0.01$) but decreased in Chinese ($P < 0.001$) cohorts.
133

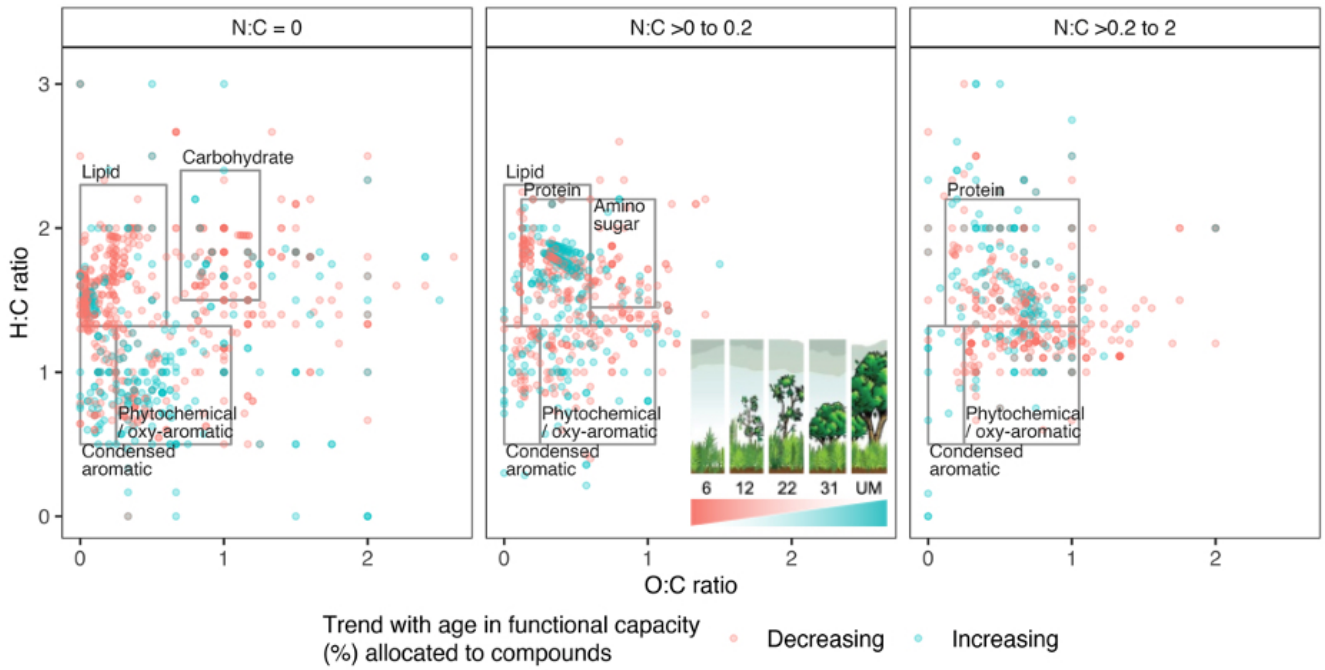

Fig. 1 | Compound-wide trend analysis results from restoration chronosequence soil (US) metagenomes. Points represent carbon-containing compounds with decreased† (aqua, *n* = 720) or increased† (red, *n* = 1,255) potential metabolism with ecosystem degradation (†trends with ecosystem degradation are interpreted as the opposite to displayed trends with revegetation age). Each compound is mapped via its chemical formula O:C, H:C and N:C elemental ratios, where clusters of points indicate energetically and chemically similar compounds. The O:C by H:C panels display a limited extent to emphasize data-rich regions. N:C ratios are displayed as three panels to represent the third dimension. Rectangular zones denoting compound classes offer a visual guide only, adapted from[49, 50]. Chrosequence samples[45] spanned planting ages 6, 12, 22, 31 years and unmined (UM), n = groups of 3.

The compound-wide trend analyses in T2D Swedish and Chinese cohorts found substantially more compounds with decreased potential metabolism in the Chinese cohort (compounds and trend data are in Supplementary Material files; carbon-containing compounds are visualized in Supplementary Figs. 34-35). In the T2D (SWE) data, 1269 compounds had trending potential

149 metabolism (n = 911 decreased, *n* = 358 increased). For the T2D (CHN) data a total of 4292
150 compounds showed trending potential metabolism (*n* = 3984 decreased, *n* = 308 increased). We note,
151 to explore the most interesting (potentially significant) results, the T2D compound-wide associations
152 were not subject to *P*-adjustment. From visual inspection, the chemical ratio mapping (Supplementary
153 Figs. 34-35) showed limited commonality in CPP trends in the vicinity of carbohydrates and
154 widespread reduced CPP in the T2D (CHN) dataset.
155
156 **Consistent trends with ecosystem degradation and T2D**
157 In the 30 selected compounds, we found consistent CPP trends with ecosystem degradation and T2D in
158 the chronosequence soils (US), T2D (SWE), and T2D (CHN) datasets, for increased potential
159 metabolism in D-fructose and L-arabinose, and decreased potential metabolism in lignin
160 (Supplementary Table 2).
161 From overlapping compound-wide trend results from the chronosequence soils (US) and T2D
162 (SWE) datasets, based on matching ModelSEED compound identifiers, 304 compounds displayed CPP
163 trends in both datasets (detailed in Supplementary Material files), from which 286 carbon-containing
164 compounds were visualized in Fig. 2. There, we observed two prominent clusters along straight lines in
165 chemical mapping space: 'Sugars' (L-arabinose, melibiose, manninotriose, D-lyxulose, sucrose,
166 D-fructose) that showed increased CPP with T2D (SWE) and ecosystem degradation (US)
167 (Supplementary Table 3); and 'BCFA-ACPs' comprising 35 compounds dominated by branched-chain
168 fatty acid (BCFA) – acyl-carrier proteins (ACPs) (Supplementary Table 4), that showed reduced CPP
169 with T2D (SWE) and ecosystem degradation (US). Importantly, the BCFA-ACPs were all involved in
170 fatty acid biosynthesis and dominated by monomethyl unsaturated (-enoyl) BCFAs that were not found
171 elsewhere in the datasets beyond this trend group. The Sugars and BCFA-ACPs are described in detail

172 in Supplementary Material Supporting Information, Supplementary Figs. 36-40, and trends shown in

173 Fig. 3.

174

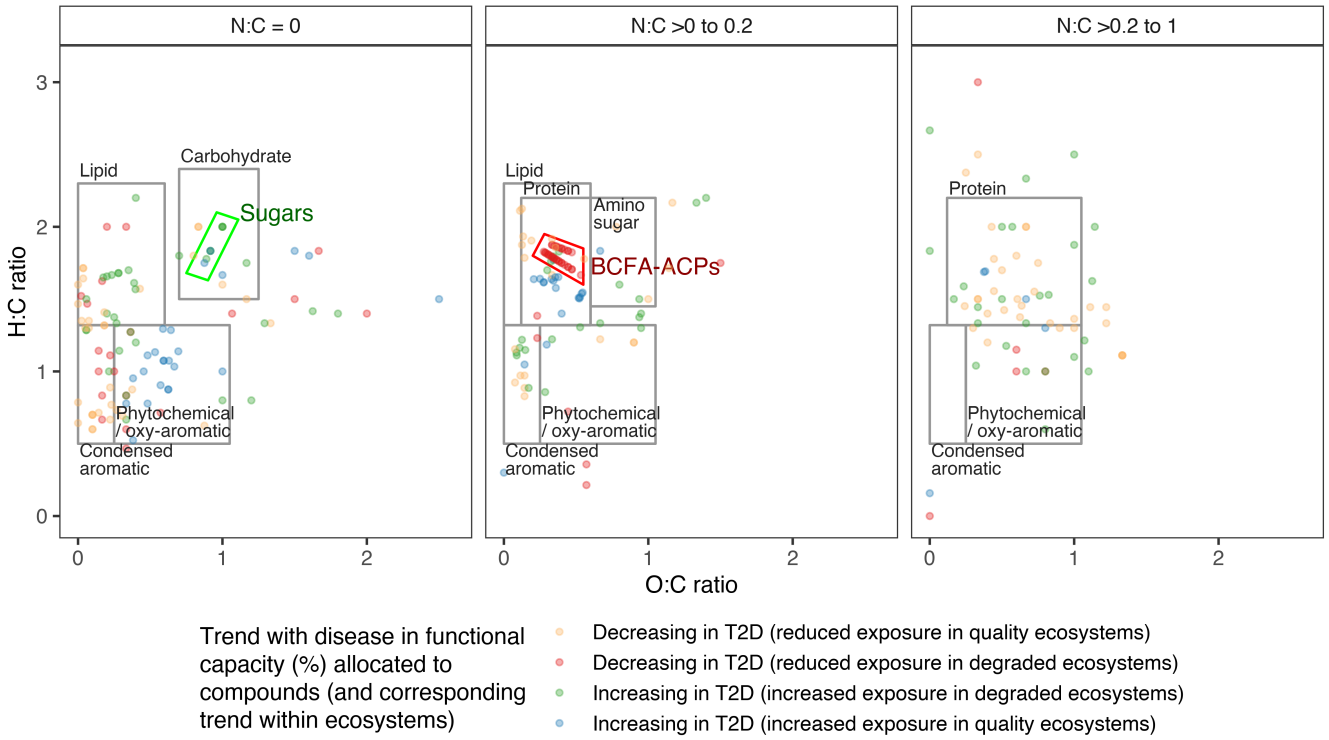

175

176 **Fig. 2 | Overlapping compound-wide trend results from restoration chronosequence soils (US)**

177 **and Swedish (SWE) T2D cohort.** Chemical ratio mapping of carbon-containing compounds with

178 overlapping potential metabolism trends from Fig. 1 and Supplementary Fig. 34). Clusters of each

179 color represent energetically and chemically similar compounds occurring in each of the four trend

180 groups shown. Total (and carbon-containing) compounds in the four trend groups are: decreased

181 potential metabolism with T2D (SWE) and ecosystem degradation, n = 70 (n = 66 red points);

182 increased potential metabolism with T2D (SWE) and ecosystem degradation, n = 89 (n = 81 green

183 points); decreased potential metabolism with T2D (SWE) and ecosystem restoration, n = 95 (n = 90

184 orange points); increased potential metabolism with T2D (SWE) and ecosystem restoration, n = 50 (n =

49 blue points). Expanded views of 'Sugars' and 'BCFA-ACPs' (i.e., branched-chain fatty acid - acyl-carrier proteins) are in Supplementary Figs. 36, 38. The plot format is further described in Fig. 1.

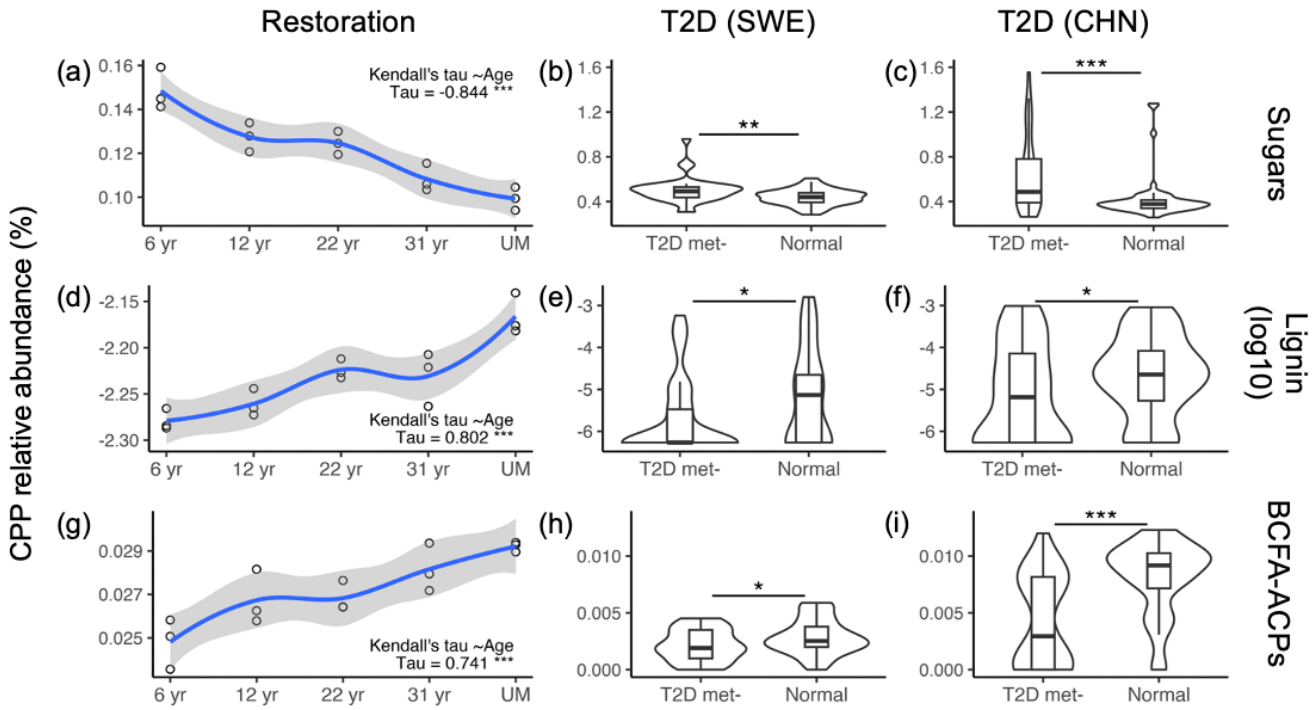

Fig. 3 | Key potential metabolism trends. Sugars (a-c), lignin (d-f), and branched-chain fatty acid – acyl carrier proteins (BCFA-ACPs, listed in Supplementary Tables 4-5) (g-i), within the restoration chronosequence (US; spanning planting ages 6, 12, 22, 31 years and unmined, UM, *n* = groups of 3) (a, d, g), T2D (Swedish cohort, SWE; T2D met- = type 2 diabetes not treated with metformin, *n* = 33; Normal = normal healthy subjects, *n* = 43) (b, e, h), and T2D (Chinese cohort, CHN; T2D met- *n* = 30; Normal *n* = 52) (c, f, i). Sugars and BCFA-ACPs were groupings identified via matching trends in T2D (SWE) and with ecosystem degradation (Fig. 2). Sugars were graphed as the sum of compound processing potential (CPP, %) for six compounds (L-arabinose, melibiose, D-fructose, sucrose, manninotriose and D-lyxulose), however subsequent testing showed only three of these sugars (L-

199 arabinose, melibiose, D-fructose) displayed individual trends in T2D (Chinese cohort, CHN)
200 (Supplementary Table 3). Lignin CPP values were $\log_{10}$-transformed to improve display.
201
202 Further matching of parallel compound-wide association trends across chronosequence soils
203 (US), T2D (SWE) and T2D (CHN) datasets identified 76 compounds, with $n = 60$ decreased, $n = 16$
204 increased CPP with ecosystem degradation T2D (Fig. 4; see Supplementary Material files). Even after
205 filtering due to intersecting the T2D (CHN) dataset, the increased CPP for sugars: L-arabinose,
206 melibiose, D-fructose still remained as trending, together with 6-phosphosucrose, an intermediate in
207 sucrose biosynthesis. The signals of decreased potential metabolism for lignin and all 35 BCFA-ACPs
208 also remained.
209 Lastly, corroboration of the majority of observed overlapping trends was found in the disturbed
210 versus natural AMI soils dataset. In disturbed AMI soils, we observed increased potential metabolism
211 of L-arabinose, D-fructose, melibiose and 6-phosphosucrose, and decreased potential metabolism of
212 lignin and all 35 of the BCFA-ACPs (all $P = <0.001$; Supplementary Fig. 41). From the 76 compounds
213 with matching potential metabolism trends with ecosystem degradation (US), T2D (SWE) and T2D
214 (CHN), a total of 65 compounds (85.5 %) displayed shared potential metabolism trends in the AMI
215 disturbed soils (Supplementary Table 5).

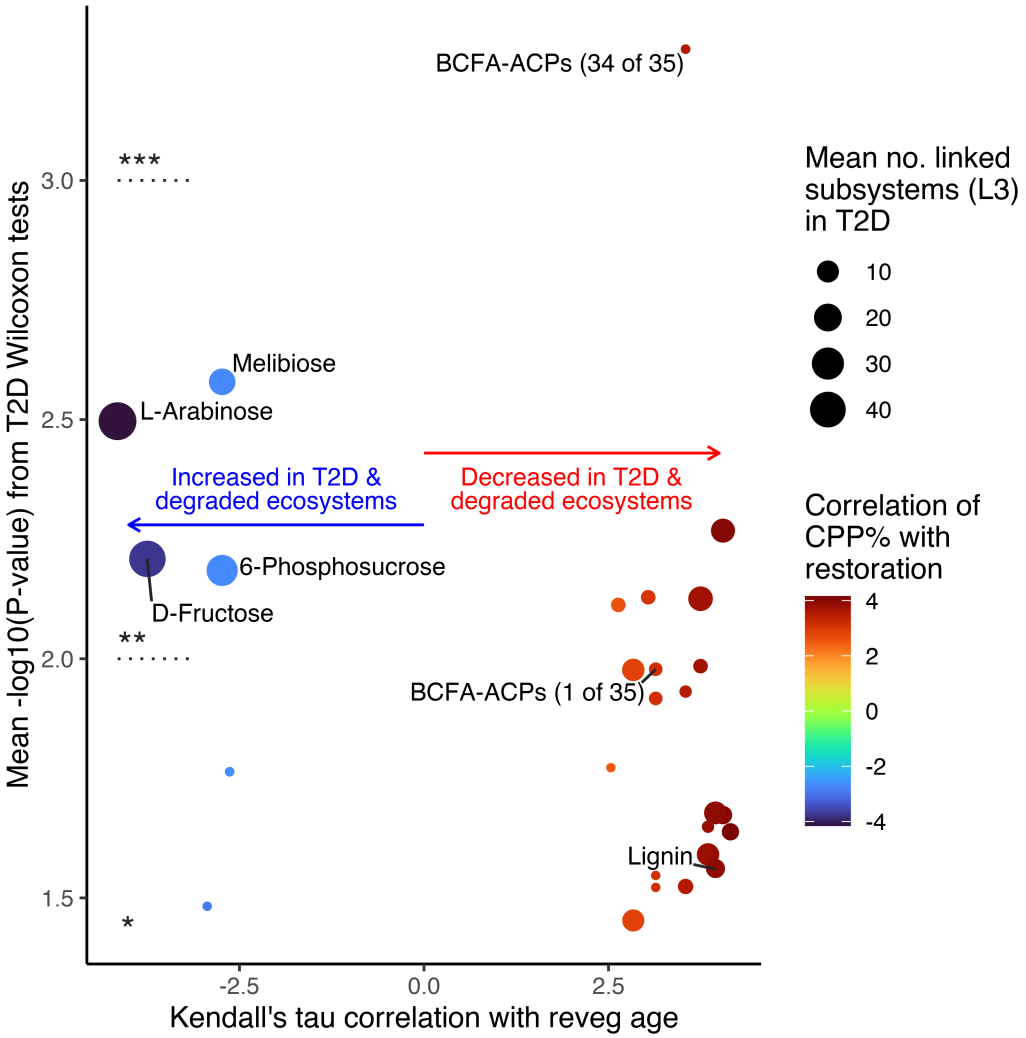

Fig. 4 | Relative importance of compounds with consistent trends across restoration chronosequence soils (US) and T2D (Swedish and Chinese) datasets. Points indicate increased or decreased potential metabolism (or compound processing potential, CPP) with ecosystem degradation (soil) and in T2D (gut) microbiomes. Compounds including branched-chain fatty acid-acyl carrier proteins (BCFA-ACPs), sugars that feature widely across many functional themes and pathways, and lignin are highlighted in the plot. Trends with ecosystem degradation are interpreted as the inverse of restoration (based on Kendall's tau ordinal correlation with revegetation age classes). Measures of significance (y-axis) from the Wilcoxon difference testing of CPP in T2D (versus normal), and the number of level 3 (L3) subsystems (functional themes) linked to each compound, are calculated as

226 mean values from the Swedish and Chinese cohorts. Details for all n = 76 compounds are in
227 Supplementary Table 5.
228

229 ## Discussion

230 We identified biologically relevant overlapping trends in the potential metabolism of compounds
231 within soil and human gut microbiomes, supporting the hypothesis that nutrient-depleted food (i.e., low
232 BCFA and lignin content, high sugar content) and/or excessive microbiome exposures associated with
233 degraded ecosystem soil may contribute to the development of type 2 diabetes. These linkages warrant
234 further investigation due to the rising burden of T2D and increasing global change impacts on soil
235 microbiomes – which underpin food quality and shape human gut microbiomes. An alternative or
236 complementary explanation may be that similar ecological stresses and dysfunction in soil and gut
237 ecosystems may be driving convergence in microbiome functional traits. Our compound-oriented
238 approach facilitates linkages to a wealth of published literature that links chemical compounds with
239 metabolism, health and wider biological processes in humans and the environment. Also, mapping of
240 compounds into the bioenergetically informed O:C, H:C and N:C coordinate space helped to reveal
241 meaningful patterns of simultaneously trending compounds (i.e., sugars, BCFA-ACPs) with soil-
242 ecosystem quality and T2D versus normal health. Our results align with the One Health framework,
243 revealing plausible functional linkages between ecosystem condition and human metabolic health, via
244 the microbiome. This work contributes necessary research towards finding synergies and co-benefits in
245 simultaneously advancing UN Sustainable Development Goals, including improving theoretical models
246 of nature–human health relationships[51, 52].
247

248 **Do branched-chain fatty acids connect healthy ecosystems and healthy people?**

249 Our results suggest that microbiomes in degraded ecosystems and T2D have reduced capacity for
250 monomethyl BCFA (mmBCFA) biosynthesis. This may reflect a shift in the biochemical composition
251 of bacterial assemblages as mmBCFAs are key components that enhance bacterial membrane fluidity,
252 and mmBCFA synthesis capacity enables membrane fluidity-related adaptive responses for survival
253 and proliferation through environmental stresses[53, 54]. BCFA levels vary among bacterial taxa, being
254 commonly higher in Gram-positive bacteria, present in some Gram-negative species, and especially
255 high in *Bacillus* and *Bifidobacterium*[53, 55]. Within ecosystems, BCFAs are present in lipid/waxy plant
256 compounds, animal (including human) tissues and fluids, ruminant products (milk, cheese, meat), fish,
257 organs, blood serum, skin, hair, adipose tissue, colostrum, breast milk, *vernix caseosa* of newborns, and
258 at very high levels in saprotrophic fungi such as *Conidiobolus* spp. found in soil and decaying organic
259 matter[54, 56, 57]. Therefore, variation in BCFA synthesis capacity could result from changes in microbial
260 taxonomic composition as ecosystems degrade.

261 Monomethyl BCFAs possess multiple beneficial bioactivities for human health and link
262 bacterial and human physiology[56]. Beneficial bioactivities of mmBCFA include lipid-lowering,
263 reducing metabolic disorder risk, maintaining normal insulin-producing β cell function and insulin
264 sensitivity, anti-inflammation, cytotoxicity to cancer cells and regulation of development[54, 55, 56].
265 Bacterially-derived mmBCFAs facilitate direct biochemical uptake and cross-domain metabolism
266 between the gut microbiome and animal hosts[58, 59, 60]. In the nematode *Caenorhabditis elegans* and
267 mammalian tissue culture cells, mmBCFA have been shown to be critical for triggering the host
268 mechanistic target of rapamycin complex 1 (mTORC1)[59, 60], a central regulator of cell growth and
269 metabolism[61]. The host mTORC1 responds to environmental signals (for example, amino acid
270 availability, growth factors, energy levels, stress) to coordinate cellular status. However, mTORC1
271 dysregulation is closely linked to diabetes, cancer, and neurodegenerative disorders[61]. Ref. [62] reported
272 high capacities for human fetal intestinal epithelial cells (enterocytes) to incorporate long-chain BCFA

273 into membrane phospholipids. Following uptake by human intestinal epithelial cells, further
274 interactions between BCFA and host endogenous BCFA synthesis and metabolism may occur[54, 56],
275 including post-translational modifications to cell proteins, which alter intestinal cell function[63]. While
276 precise mechanisms are uncertain, it is possible that mmBCFA in the gut microbiome may modulate
277 host cellular metabolism and physiological functioning via these interactions.

278 Microbial sources play a dominant role in the supply of health-associated mmBCFA[55, 56]. Key
279 inputs to BCFA synthesis include branched-chain amino acids which can only be made in bacteria,
280 plants, and fungi, but not in animals[64]; or shorter BCFA, which can be elongated. Microbes (for
281 example, rumen bacteria) also contribute to BCFA synthesis in animals[56]. Therefore, both diet and gut
282 microbiome synthesis provide major sources of BCFA to humans[55, 56]. Within soil and gut
283 microbiomes, the interchange of BCFA between substrates and microbes can be expected because fatty
284 acids are a high-value energy source, and bacteria assimilate environmental BCFA into their bodies[65,
285 66]. In the gut, the constant release of mmBCFAs will occur from cell membranes with bacterial
286 turnover from competitive interactions[67] and secretion of fatty acids and their derivatives[58]. A portion
287 of these gut bacteria may be supplied from external ecosystem exposures[21, 22], while BCFA-
288 synthesizing bacteria may be further shaped by diet and other factors (for example, high BCFA-content
289 *Bifidobacterium* spp. proliferate in infants receiving breast milk[68]).

290 As ecosystems degrade, there may be several reasons why BCFA-synthesizing organisms
291 decline. Ecosystem degradation is widely associated with reductions in soil organic matter[3, 69, 70, 71].
292 Indeed, the more degraded chronosequence soils we analyzed had lower soil organic content than
293 unmined sites[72]. Soil organic matter comprises a continuum of progressively decomposed organic
294 compounds, commonly including amino acids and fatty acids[73]. Amino acids are released from proteins
295 in the soil at rates correlated with soil organic matter pools and soil protein concentrations[74], and
296 increasing with ecosystem succession[75]. Natural decomposition and recycling networks of saprotrophic

297 fungi (including high BCFA-content spp.) may also be degraded, likely reducing BCFA content and
298 turnover in soil microbiomes. Diverse plant litter contributes to increased soil carbon, higher microbial
299 abundance, diversity, decomposition and turnover, which strengthens over time[76]. Taken together, these
300 influences may reduce access to and recycling of both branched-chain amino acids and fatty acids for
301 soil microbiomes in degraded ecosystems, thereby potentially reducing ambient human exposure to
302 health-promoting microbial mmBCFA synthesis capacity (Fig. 5). Degraded agricultural soils might
303 also produce crops and ruminant products (for example, meat, dairy) with reduced mmBCFA content,
304 that impact gut microbiomes via diet. However, these ideas require further investigation.
305

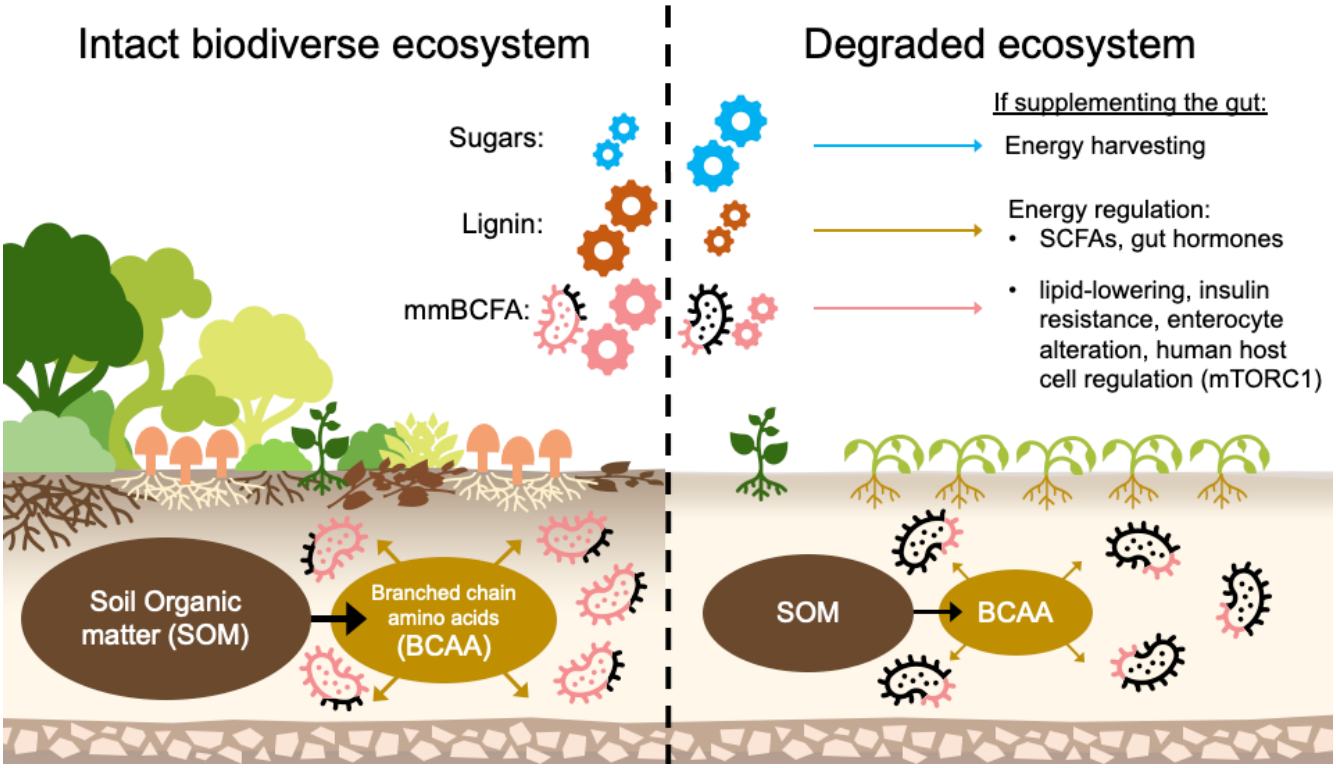

306

307 **Fig. 5 | Hypothesis linking ecosystem degradation and type 2 diabetes.** Intact natural ecosystems
308 typically have greater biodiversity, woody plant debris (including lignin), fungal recycling and soil
309 organic matter (SOM) pools. SOM releases branched-chain amino acids (BCAA) which are used to
310 make precious monomethyl branched-chain fatty acids (mmBCFA) used in bacterial cell membranes,

311 stored by fungi, and needed to regulate animal cell metabolism via the mechanistic target of rapamycin
312 complex 1 (mTORC1) among other pathways. With ecosystem degradation, soil organic matter
313 decomposes into simple sugars. Degraded soil microbiomes have increased capacity to metabolize
314 simple sugars, decreased capacity to metabolize lignin (potentially impacting production of short-chain
315 fatty acids, SCFAs), and decreased mmBCFA synthesis capacity (potentially linked to mmBCFA
316 content in microbial bodies, necromass and the wider ecosystem). If people consume nutrient-depleted
317 food (low mmBCFA and lignin content, high sugar content) and/or are increasingly exposed to soil
318 microbiomes associated with degraded ecosystems, it may contribute to metabolic shifts in the gut
319 microbiome consistent with type 2 diabetes.
320
321 **Identified compounds linked to energy harvesting**
322 We found that potential metabolism of sugars L-arabinose, D-fructose, melibiose and the intermediate
323 compound 6-phosphosucrose each increased with ecosystem degradation and T2D. Additionally, we
324 found the potential metabolism of sucrose, glucose, galactose, xylose and mannose increased in more
325 degraded ecosystems. Sugars are the most abundant organic compounds in the biosphere and are key
326 carbon and energy sources for soil microbes[77]. Sugars in soil can either be derived from primary
327 sources (for example, decomposition of plant litter, rhizodeposits, root exudates) or secondary sources
328 (for example, microorganisms and their residues)[77]. Previous work suggests that galactose, glucose,
329 mannose, arabinose and xylose are chief components of sugar residues found within soil organic
330 matter[78]. Our detection of increased potential metabolism of simple sugars (largely monosaccharides
331 and disaccharides) likely reflects enhanced microbial decomposition of soil organic matter within more
332 degraded ecosystems[69].
333 In the gut microbiome, carbohydrate metabolism contributes up to 10% of the host's overall
334 energy extraction and is recognized as an important contributor to insulin resistance and the

335 development of obesity and prediabetes[79]. Ref. [79] found increased gut microbiome metabolism of
336 monosaccharides, including fructose, galactose, mannose and xylose, significantly correlated with
337 insulin resistance. Interestingly, in soils and humans, enhanced sugar metabolism is also associated
338 with more opportunistic bacteria[80]. Increased relative abundances of opportunists (including fast-
339 growing, potential pathogens) have been associated with disturbance in urban greenspace soils[37] and in
340 human-altered land uses[81]. If microbiome components promoting enhanced sugar metabolism are
341 transferred from degraded ecosystems to the human gut, they may foster opportunistic or pathogen-like
342 traits – potentially contributing to increased energy harvest and metabolic imbalances associated with
343 T2D.

344

345 **Identified compounds linked to energy management**

346 We found altered potential metabolism for compounds with plausible links to energy storage via fatty
347 acids, gut hormone secretion and appetite regulation that decreased in both degraded ecosystems and
348 T2D. This raises the question whether nutrient-depleted foods and/or excessive exposures to degraded
349 ecosystem soils that are deficient in potential metabolism of compounds involved in energy
350 management may shape gut microbiomes that are also deficient in this way. We discuss above how gut
351 microbiome mmBCFA content and biosynthesis capacity might modulate host cellular metabolism via
352 central mTORC1 regulation, alteration of enterocyte phospholipid composition and function, and/or
353 supply of BCFA for further host endogenous fatty acid synthesis and BCFA-mediated metabolism.

354 Dietary fiber, such as lignin, is known to decrease plasma ghrelin, known as the hunger
355 hormone, and increase other key gut regulatory hormones: cholecystokinin, glucagon-like-peptide-1
356 (GLP-1), and peptide YY[82]. Short-chain fatty acids (SCFAs) are produced when gut microbes ferment
357 non-digestible fibers, and these SCFAs bind to receptors in the colon, leading to the production of
358 hormones that regulate food intake, body weight, and energy metabolism[10, 82]. Similar trends to lignin

359 appeared for sinapyl alcohol and coumaryl alcohol (both precursors to lignin) in the compound-wide
360 results spanning all datasets. Potential metabolism for the dietary fiber pectin also decreased in T2D
361 (significantly in the Swedish cohort, and marginally in the Chinese cohort), but not in degraded
362 ecosystems. We searched for oligosaccharides (for example, fructan, inulin, galactan) but did not detect
363 these compounds in our datasets. Additional compounds that we identified remain to be explored
364 (Supplementary Table S5).
365

366 **Disentangling dietary and environmental influences on T2D gut microbiomes**

367 Altered potential metabolism for compounds detected within gut microbiomes may arise from dietary
368 and environmental exposures, gut environment and functions, neurological influences, among other
369 factors[83]. Where we found matching trends across all case studies (for example, L-arabinose, D-
370 fructose, melibiose, BCFA-ACPs, lignin), this may be consistent with an alignment between
371 environmental exposures and dietary inputs. In the scenario where compounds consistently showed in
372 both T2D cohorts, but not in the restoration chronosequence soils, this suggests dietary effects alone.
373 For example, increased potential metabolism results for amylopectin suggests that excessive
374 consumption of starch-rich foods may contribute to T2D. For many compounds we found alignment in
375 potential metabolism between the ecosystem condition and T2D gut (Chinese cohort), but not the T2D
376 gut (Swedish cohort) – this may point to greater environmental exposures and detrimental health
377 influence in some population groups. Yet another contrast occurred in the case of ammonia, where
378 potential metabolism trends were opposing in the T2D cohorts, in the absence of any ecosystem
379 condition effect, which suggests influences from dietary exposures alone associating with T2D. We
380 raise further noteworthy implications for community connection to soils and ecosystems, and study
381 limitations in the Supplementary Material, Supporting Information.
382

383 **Conclusions**

384 We found overlapping trends in the potential metabolism of compounds with beneficial bioactivities,
385 and involved in energy harvesting and management, within separate model case study datasets of soil-
386 ecosystem degradation from the United States and Australia, and T2D gut microbiomes from Swedish
387 and Chinese cohorts. Our results support existing studies implicating, at least in part, roles for
388 microbiomes, sugars, lignin (dietary fiber) and mmBCFA in metabolism and T2D. Additionally, our
389 findings could inform new T2D interventions; and suggest that degraded soil microbiomes may
390 contribute to metabolic imbalances found in T2D via nutrient-depleted food (for example, low
391 mmBCFA and lignin content, high sugar content) and/or excessive environmental exposures associated
392 with degraded ecosystems. Our method used to examine microbiome potential metabolism at the
393 resolution of individual compounds has raised new biologically interpretable and testable hypotheses
394 regarding potential links between soil, ecosystem and T2D gut health that warrant further
395 transdisciplinary investigation.

396

397 ## Methods

398 **Case study data**

399 We examined previously published soil and human gut metagenome case study datasets (detailed in
400 Supplementary Table 1). Restoration chronosequence[45] soil samples spanned planting ages 6, 12, 22,
401 31 years and unmined (UM) with *n* = groups of 3. T2D datasets were from Swedish[46] (T2D *n* = 33,
402 Normal *n* = 43) and Chinese[47] (T2D *n* = 30, Normal *n* = 52) cohorts. We used metadata from ref. 12 to
403 exclude subjects treated with metformin or diagnosed with prediabetes. From the Chinese cohort, we
404 only included subjects >50 years old to compare with the mature age (69-72 years) Swedish subjects.
405 Australian Microbiome Initiative (AMI) disturbed (*n* = 29) versus natural (*n* = 55) soils were surface
406 depth (0–10 cm), from the temperate climate zone, with 7.5–45 % clay content (i.e., avoiding very

407 sandy and very clayey soils) as described in ref. 38. Disturbed soils were from agricultural land uses
408 (cereals, cotton, horticulture, irrigated pasture), while natural soils were from conservation and national
409 park land uses.
410
411 **Metagenome functional profiling via compound processing potential (CPP)**
412 Our CPP analysis approach used a purpose-built bioinformatics workflow (Fig. 6) that redistributes
413 values of functional potential relative abundances (%), from the scale of functions (i.e., biochemical
414 pathways that often comprise multiple linked chemical reactions), down to the level of individual
415 chemical compounds. These compounds are conceptually participating in a weighted array of
416 intersecting chemical reactions that represent the collective functional capacity of a metagenome.
417

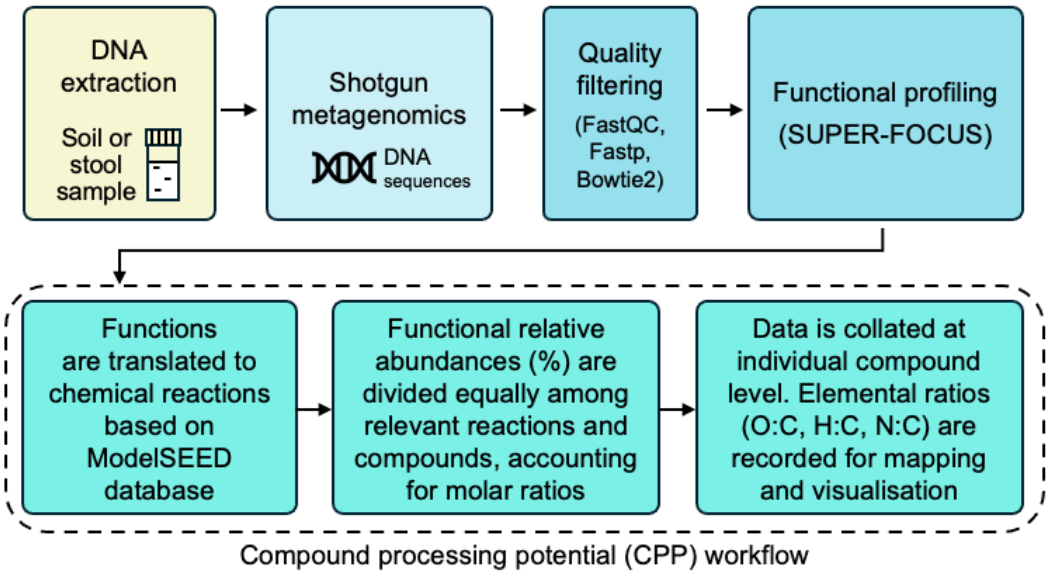

418
419 **Fig. 6 | Overview of the compound processing potential (CPP) analysis workflow.** Metagenomic
420 functional potential pathway relative abundances were translated to quantify hypothetical potential
421 metabolism at the scale of individual compounds. CPP % values for carbon-containing compounds can
422 be mapped using chemical formula ratios to visualize clusters of bioenergetically similar compounds
423 that trend together.

Measures of CPP were derived via steps outlined in Fig. 6. Firstly, following ref. 38, using high performance computing resources[84, 85] raw metagenomic sequences were accessed, trimmed for quality control, and human case study sequences that mapped using Bowtie2[86] to the human genome (GRCh38.p14/hg38) were excluded (low levels were observed; Supplementary Material, Supporting Information). Then good quality read 1 sequences were classified to SEED subsystem[87] functional annotations and relative abundances using SUPER-FOCUS software[88]. Every SUPER-FOCUS function (output row) was translated to one or more corresponding chemical reaction(s) using a purpose-built R-script algorithm based on ModelSEED database lookup tables (from https://github.com/ModelSEED/ModelSEEDDatabase; accessed 10 Aug 2022). Linking of functions (and sub-functions where present) to chemical reactions was based on either: full matching of functional hierarchies (using subsystem-class, -subclass, -name and -role); detection of Enzyme Commission (EC) number; or matching of SUPER-FOCUS function name within ModelSEED lookup tables for reactions (reaction name or alias), subsystems (role), or reaction-pathways (external reaction name). Reactions were then linked to corresponding compounds using ModelSEED database tables ('reactions.tsv', 'compounds.tsv').

Advancing from the previous method used in ref. 38, here we derived CPP measures at the resolution of individual compounds (all software parameters and supporting R code for CPP calculations are available at: https://github.com/liddic/cpp3d_t2d):

(1) Function level relative abundances from SUPER-FOCUS (which sum to 100% in each sample) were allocated to compounds by dividing values equally across all sub-functions and reactions, and dividing again across all corresponding compounds, with weightings to account for stoichiometric coefficients for each compound within each reaction, with equal consideration to reactants and products.

448 (2) Relative abundances (%) for respective unique compounds (which may arise across multiple
449 reactions and functions) were then collated and summed to provide a summary CPP relative
450 abundance (%) for each compound. (Here, conversion to CPP data format successfully
451 recovered typically 65 to 70% of the initial 100% function potential per sample; Supplementary
452 Table 1).
453 (3) For mapping visualization of CPP patterns for carbon-containing compounds, elemental ratios
454 of O:C, H:C, and N:C were calculated. Such chemical mapping frameworks have been used to
455 display and interpret groupings of energetically and chemically similar compounds[38, 49].
456

457 **Statistical Analysis**

458 We used a staged approach to explore overlapping potential metabolism (i.e., CPP) trends in the soil
459 and T2D gut samples. We progressively examined the restoration chronosequence soils (US), then
460 Swedish and Chinese T2D cohorts, and lastly the AMI soils to corroborate findings. Further detail is in
461 Supplementary Material and at https://github.com/liddic/cpp3d_t2d:
462 (1) ***Thirty selected compounds*** were initially explored for CPP trends, chosen due to their
463 relevance to soil and/or gut health (Supplementary Table 2). In chrosequence soils (US), CPP
464 trends were evaluated using Kendall's tau rank correlation tests based on ordinal revegetation
465 age classes. We interpreted CPP trends with ecosystem degradation as the inverse of calculated
466 trends with increasing revegetation age (as informed by previous work showing highly
467 disturbed post-mining soil microbiomes progressively shift in their structure with ecosystem
468 restoration towards intact natural condition[36]). In T2D versus normal health, CPP trends (i.e.,
469 differences) were evaluated using non-parametric Wilcoxon rank-sum (Mann-Whitney) tests,
470 due to often differing variance of groups (T2D vs. normal) and to avoid normality assumptions.
471 All data were plotted to assist interpretation.

472 (2) ***Compound-wide association tests*** were also performed to exhaustively scan CPP trends for all
473 compounds. This used the same approach as above, with further steps to automate analyses. In
474 correlation testing of chrosequence soils, compounds that did not have relative abundance data
475 for at least a quarter of the total sample number were excluded due to low data. In this
476 chrosequence soil dataset, strong CPP trends were discovered, and only significant results based
477 on Benjamini and Hochberg adjusted *P*-values were considered further. In the subsequent
478 compound-wide association analysis of T2D gut samples, compounds were only included if at
479 least one or other of the T2D or normal groups contained at least 50% non-zero CPP values.
480 Testing was based on $\log_{10}$-transformed CPP % values, after zero replacement with small
481 positive values equal to half the minimum non-zero CPP % of all samples. One-sided
482 (directional) difference tests were based on whether the median value in T2D was greater or
483 less than the median value for normal healthy subjects. To retain and explore the most
484 interesting (potentially significant) results from the compound-wide T2D analyses, these data
485 were not subject to *P*-adjustment for multiple testing.
486 (3) ***Overlap analysis.*** Compounds with CPP % trends in both the restoration chronosequence (US)
487 and T2D (SWE) case studies were identified, based on matching ModelSEED compound
488 identifiers. Our focus was to highlight compounds that displayed consistent increased or
489 decreased CPP values with ecosystem degradation and T2D.
490 (4) ***Visualising compound-wide association test results.*** Compounds with CPP % trends in the
491 restoration chronosequence (US) and T2D (SWE) gut microbiomes, and overlaps between the
492 two, were mapped using their chemical formula elemental ratios of O:C, H:C, and N:C. From
493 this mapping space, prominent localized clusters of consistently trending compounds (i.e., with
494 ecosystem degradation and T2D) were identified and further analyzed to determine trends in
495 their collective (summed) CPP % and to interpret their possible metabolic importance.

496 (5) ***Trend consolidation and validation.*** The above steps were repeated with the second T2D
497 (CHN) cohort, which refined the list of compounds with parallel CPP trends with ecosystem
498 degradation (US) and in both T2D datasets. Trend and contextual information for these
499 compounds was reported and visualized to represent the significance (-$\log_{10}$[*P*-value]; as used
500 in genome-wide association study Manhattan plots) of association with ecosystem degradation
501 and T2D, and the number of functional themes (level 3 subsystems) they are linked to. Here,
502 data for T2D were visualized using mean results from the Swedish and Chinese cohort datasets.
503 To corroborate parallel CPP trends from the restoration chronosequence (US) and both T2D
504 datasets, a focused analysis of CPP trends only for previously identified compounds was
505 performed using the disturbed versus natural AMI soils.
506 (6) ***Beta diversity ordinations.*** Supplementary analyses using the restoration chronosequence (US)
507 and T2D Swedish cohort dataset were performed to examine community-scale compositional
508 patterns and differences between sample groups and analysis approaches, comparing
509 conventional functional potential (%) data (termed 'functions') versus CPP (%) data. This
510 analysis used principal coordinate analysis (PCoA) ordinations based on Bray-Curtis distances,
511 and testing for differences between groups via permutational analysis of variance
512 (PERMANOVA) and beta dispersion testing for homogeneity of groupings using the vegan R
513 package[89]. These data are presented in the Supplementary Material, Supporting Information and
514 Supplementary Fig. 42.
515
516

517 **Data availability**

518 The datasets used are available from NCBI Sequence Read Archive (accessions PRJEB1786 and
519 PRJNA422434), MG-RAST (project mgp16379), and soil metagenomes from the Australian
520 Microbiome Initiative data portal (https://data.bioplatforms.com/organization/australian-microbiome).

521

522 **Code availability**

523 Code used to support this study is available from: https://github.com/liddic/cpp3d_t2d .

524

525 **Acknowledgments**

526 We acknowledge and thank the authors of previously published metagenomics datasets used here,
527 which enabled comparison of samples spanning human and environmental health. This includes the
528 Australian Microbiome initiative which was supported by funding from Bioplatforms Australia and the
529 Integrated Marine Observing System (IMOS) through the Australian Government's National
530 Collaborative Research Infrastructure Strategy (NCRIS), Parks Australia through the Bush Blitz
531 program funded by the Australian Government and BHP, and the CSIRO. We acknowledge Indigenous
532 peoples and the traditional custodians of the lands on which the case study datasets originate, and our
533 authors live and work. This work was supported by the People, Cities and Nature research program
534 (Aotearoa New Zealand Ministry of Business, Innovation and Employment, grant UOWX2101).

535

References

1. Muhummed, A.M., Lanker, K.C., Yersin, S., Zinsstag, J. & Vonaesch, P. One Health, One Microbiome. *Microbiome* **13**, 216 (2025).

2. Banerjee, S. & van der Heijden, M.G.A. Soil microbiomes and one health. *Nature Reviews Microbiology* **21**, 6-20 (2022).

3. IPBES. The IPBES assessment report on land degradation and restoration. Bonn, Germany; 2018.

4. Pearson, E.R. Type 2 diabetes: a multifaceted disease. *Diabetologia* **62**, 1107-1112 (2019).

5. Beulens, J.W.J. *et al.* Environmental risk factors of type 2 diabetes—an exposome approach. *Diabetologia* **65**, 263-274 (2022).

6. Lu, X. *et al.* Type 2 diabetes mellitus in adults: pathogenesis, prevention and therapy. *Signal Transduction and Targeted Therapy* **9**, 262 (2024).

7. Ong, K.L. *et al.* Global, regional, and national burden of diabetes from 1990 to 2021, with projections of prevalence to 2050: a systematic analysis for the Global Burden of Disease Study 2021. *The Lancet* **402**, 203-234 (2023).

8. Sun, H. *et al.* IDF Diabetes Atlas: Global, regional and country-level diabetes prevalence estimates for 2021 and projections for 2045. *Diabetes Res Clin Pract* **183**, 109119 (2022).

9. Daisley, B.A. *et al.* Emerging connections between gut microbiome bioenergetics and chronic metabolic diseases. *Cell Reports* **37**, 110087 (2021).

10. Chao, J., Coleman, R.A., Keating, D.J. & Martin, A.M. Gut Microbiome Regulation of Gut Hormone Secretion. *Endocrinology* **166** (2025).

11. Rowland, I. *et al.* Gut microbiota functions: metabolism of nutrients and other food components. *European Journal of Nutrition* **57**, 1-24 (2018).

12. Forslund, K. *et al.* Disentangling type 2 diabetes and metformin treatment signatures in the human gut microbiota. *Nature* **528**, 262-266 (2015).

13. Chen, L. *et al.* Fecal microbiota transplantation ameliorates type 2 diabetes via metabolic remodeling of the gut microbiota in db/db mice. *BMJ Open Diabetes Research & Care* **11**, e003282 (2023).

14. Wu, Z. *et al.* Fecal microbiota transplantation reverses insulin resistance in type 2 diabetes: A randomized, controlled, prospective study. *Frontiers in Cellular and Infection Microbiology* **Volume 12 - 2022** (2023).

15. Gilbert, J.A. *et al.* Current understanding of the human microbiome. *Nature Medicine* **24**, 392 (2018).

16. Wopereis, H., Oozeer, R., Knipping, K., Belzer, C. & Knol, J. The first thousand days – intestinal microbiology of early life: establishing a symbiosis. *Pediatric Allergy and Immunology* **25**, 428-438 (2014).

17. Attard, S.M. *et al.* Multilevel examination of diabetes in modernising China: what elements of urbanisation are most associated with diabetes? *Diabetologia* **55**, 3182-3192 (2012).

18. Cheema, A., Adeloye, D., Sidhu, S., Sridhar, D. & Chan, K.Y. Urbanization and prevalence of type 2 diabetes in Southern Asia: A systematic analysis. *J Glob Health* **4**, 010404 (2014).

19. Ruiz-Alejos, A. *et al.* Addressing the impact of urban exposure on the incidence of type 2 diabetes mellitus: The PERU MIGRANT Study. *Scientific Reports* **8**, 5512 (2018).

20. Gassasse, Z., Smith, D., Finer, S. & Gallo, V. Association between urbanisation and type 2 diabetes: an ecological study. *BMJ Global Health* **2**, e000473 (2017).

21. Roslund, M.I. *et al.* Long-term biodiversity intervention shapes health-associated commensal microbiota among urban day-care children. *Environment International* **157**, 106811 (2021).

22. Rothschild, D. *et al.* Environment dominates over host genetics in shaping human gut microbiota. *Nature* **555**, 210 (2018).

23. Anthony, M.A., Bender, S.F. & van der Heijden, M.G.A. Enumerating soil biodiversity. *Proceedings of the National Academy of Sciences* **120**, e2304663120 (2023).

24. Blakemore, R.J. Biodiversity restated: > 99.9% of global species in Soil Biota. *ZooKeys* **1224**, 283-316 (2025).

25. Zhou, G.-L. *et al.* Exposure to greenspaces sourced soils improves mice gut microbiota. *Environmental Pollution* **362**, 124931 (2024).

26. Liu, W. *et al.* Exposure to soil environments during earlier life stages is distinguishable in the gut microbiome of adult mice. *Gut Microbes* **13**, 1-13 (2021).

27. Liddicoat, C. *et al.* Naturally-diverse airborne environmental microbial exposures modulate the gut microbiome and may provide anxiolytic benefits in mice. *Science of The Total Environment* **701**, 134684 (2020).

28. Grieneisen, L.E. *et al.* Genes, geology and germs: gut microbiota across a primate hybrid zone are explained by site soil properties, not host species. *Proceedings of the Royal Society B: Biological Sciences* **286**, 20190431 (2019).

29. Cao, T., Luo, Y., Shi, M., Tian, X. & Kuzyakov, Y. Microbial interactions for nutrient acquisition in soil: Miners, scavengers, and carriers. *Soil Biology and Biochemistry* **188**, 109215 (2024).

30. Adamczyk, B. How do terrestrial plants access high molecular mass organic nitrogen, and why does it matter for soil organic matter stabilization? *Plant and Soil* (2021).

31. Qin, W., Song, P. & Zhang, S. Seasonal and Soil Microbiota Effects on the Adaptive Strategies of Wild Goitered Gazelles Based on the Gut Microbiota. *Frontiers in Microbiology* **Volume 13 - 2022** (2022).

32. Peng, H. *et al.* Longitudinal gut microbiota tracking reveals the dynamics of horizontal gene transfer. *Nature Communications* **16**, 11543 (2025).

33. Bindels, L.B. *et al.* A blueprint for contemporary studies of microbiomes. *Microbiome* **13**, 95 (2025).

34. Finley, B.K. *et al.* Unraveling the influence of microbial necromass on subsurface microbiomes: metabolite utilization and community dynamics. *ISME Communications* **5** (2025).

35. Roslund, M.I., Laitinen, O.H. & Sinkkonen, A. Scoping review on soil microbiome and gut health—Are soil microorganisms missing from the planetary health plate? *People and Nature* **6**, 1078-1095 (2024).

36. Liddicoat, C. *et al.* Next generation restoration metrics: Using soil eDNA bacterial community data to measure trajectories towards rehabilitation targets. *Journal of Environmental Management* **310**, 114748 (2022).

37. Delgado-Baquerizo, M. *et al.* Global homogenization of the structure and function in the soil microbiome of urban greenspaces. *Science Advances* **7**, eabg5809 (2021).

38. Liddicoat, C. *et al.* Bioenergetic mapping of 'healthy microbiomes' via compound processing potential imprinted in gut and soil metagenomes. *Science of The Total Environment* **940**, 173543 (2024).

39. Sun, X. *et al.* Unforeseen high continental-scale soil microbiome homogenization in urban greenspaces. *Nature Cities* **2**, 759-769 (2025).

40. Van Hul, M. *et al.* What defines a healthy gut microbiome? *Gut* **73**, 1893 (2024).

41. Fierer, N., Wood, S.A. & Bueno de Mesquita, C.P. How microbes can, and cannot, be used to assess soil health. *Soil Biology and Biochemistry* **153**, 108111 (2021).

42. Neveu, V., Nicolas, G., Amara, A., Salek, R.M. & Scalbert, A. The human microbial exposome: expanding the Exposome-Explorer database with gut microbial metabolites. *Scientific Reports* **13**, 1946 (2023).

43. Mallick, H. *et al.* Predictive metabolomic profiling of microbial communities using amplicon or metagenomic sequences. *Nature Communications* **10**, 3136 (2019).

44. Garza, D.R., van Verk, M.C., Huynen, M.A. & Dutilh, B.E. Towards predicting the environmental metabolome from metagenomics with a mechanistic model. *Nature Microbiology* **3**, 456-460 (2018).

45. Sun, S. & Badgley, B.D. Changes in microbial functional genes within the soil metagenome during forest ecosystem restoration. *Soil Biology and Biochemistry* **135**, 163-172 (2019).

46. Karlsson, F.H. *et al.* Gut metagenome in European women with normal, impaired and diabetic glucose control. *Nature* **498**, 99-103 (2013).

47. Qin, J. *et al.* A metagenome-wide association study of gut microbiota in type 2 diabetes. *Nature* **490**, 55-60 (2012).

48. Bissett, A. *et al.* Introducing BASE: the Biomes of Australian Soil Environments soil microbial diversity database. *GigaScience* **5**, 21 (2016).

49. Rivas-Ubach, A. *et al.* Moving beyond the van Krevelen Diagram: A New Stoichiometric Approach for Compound Classification in Organisms. *Analytical Chemistry* **90**, 6152-6160 (2018).

50. Wu, X. *et al.* Microbial Interactions With Dissolved Organic Matter Drive Carbon Dynamics and Community Succession. *Frontiers in Microbiology* **9** (2018).

51. Fisher, B. *et al.* Can nature deliver on the sustainable development goals? *The Lancet Planetary Health* **3**, e112-e113 (2019).

52. Marselle, M.R. *et al.* Pathways linking biodiversity to human health: A conceptual framework. *Environment International* **150**, 106420 (2021).

53. Yoon, Y., Lee, H., Lee, S., Kim, S. & Choi, K.-H. Membrane fluidity-related adaptive response mechanisms of foodborne bacterial pathogens under environmental stresses. *Food Research International* **72**, 25-36 (2015).

54. Gozdzik, P., Magkos, F., Sledzinski, T. & Mika, A. Monomethyl branched-chain fatty acids: Health effects and biological mechanisms. *Progress in Lipid Research* **90**, 101226 (2023).

55. Yang, S.-j., Yu, X.-k. & Zuo, Q. Branched- Chain Fatty Acids and Obesity: A Narrative Review. *Nutrition Reviews* (2025).

56. Mao, S. *et al.* Branched-Long-Chain Monomethyl Fatty Acids: Are They Hidden Gems? *Journal of Agricultural and Food Chemistry* **71**, 18674-18684 (2023).

57. Maheshwari, G. *et al.* Branched-Chain Fatty Acids as Mediators of the Activation of Hepatic Peroxisome Proliferator-Activated Receptor Alpha by a Fungal Lipid Extract. *Biomolecules* **10** (2020).

58. Brown, E.M., Clardy, J. & Xavier, R.J. Gut microbiome lipid metabolism and its impact on host physiology. *Cell Host & Microbe* **31**, 173-186 (2023).

59. Zhu, M. *et al.* Monomethyl branched-chain fatty acid mediates amino acid sensing upstream of mTORC1. *Developmental Cell* **56**, 2692-2702.e2695 (2021).

60. Zhu, H., Shen, H., Sewell, A.K., Kniazeva, M. & Han, M. A novel sphingolipid-TORC1 pathway critically promotes postembryonic development in Caenorhabditis elegans. *eLife* **2**, e00429 (2013).

61. Takahara, T., Amemiya, Y., Sugiyama, R., Maki, M. & Shibata, H. Amino acid-dependent control of mTORC1 signaling: a variety of regulatory modes. *Journal of Biomedical Science* **27**, 87 (2020).

62. Liu, L. *et al.* Human fetal intestinal epithelial cells metabolize and incorporate branched chain fatty acids in a structure specific manner. *Prostaglandins, Leukotrienes and Essential Fatty Acids* **116**, 32-39 (2017).

63. Ezzine, C. *et al.* Fatty acids produced by the gut microbiota dampen host inflammatory responses by modulating intestinal SUMOylation. *Gut Microbes* **14**, 2108280 (2022).

64. Neinast, M., Murashige, D. & Arany, Z. Branched Chain Amino Acids. *Annual Review of Physiology* **81**, 139-164 (2019).

65. Sen, S. *et al.* Growth-Environment Dependent Modulation of Staphylococcus aureus Branched-Chain to Straight-Chain Fatty Acid Ratio and Incorporation of Unsaturated Fatty Acids. *PLOS ONE* **11**, e0165300 (2016).

66. Yao, J. & Rock, C.O. How Bacterial Pathogens Eat Host Lipids: Implications for the Development of Fatty Acid Synthesis Therapeutics*. *Journal of Biological Chemistry* **290**, 5940-5946 (2015).

67. Booth, S.C., Smith, W.P.J. & Foster, K.R. The evolution of short- and long-range weapons for bacterial competition. *Nature Ecology & Evolution* **7**, 2080-2091 (2023).

68. Stewart, C.J. *et al.* Temporal development of the gut microbiome in early childhood from the TEDDY study. *Nature* **562**, 583-588 (2018).

69. Chen, S. *et al.* Plant diversity enhances productivity and soil carbon storage. *Proceedings of the National Academy of Sciences* **115**, 4027 (2018).

70. Kooch, Y., Amani, M. & Abedi, M. The effect of shrublands degradation intensity on soil organic matter-associated properties in a semi-arid ecosystem. *Science of The Total Environment* **853**, 158664 (2022).

71. Cunningham, S.C. *et al.* Reforestation with native mixed-species plantings in a temperate continental climate effectively sequesters and stabilizes carbon within decades. *Global Change Biology* **21**, 1552-1566 (2015).

72. Avera, B.N., Strahm, B.D., Burger, J.A. & Zipper, C.E. Development of ecosystem structure and function on reforested surface-mined lands in the Central Appalachian Coal Basin of the United States. *New Forests* **46**, 683-702 (2015).

73. Song, Y. *et al.* Soil metabolomics: Deciphering underground metabolic webs in terrestrial ecosystems. *Eco-Environment & Health* **3**, 227-237 (2024).

74. Näsholm, T., Kielland, K. & Ganeteg, U. Uptake of organic nitrogen by plants. *New Phytologist* **182**, 31-48 (2009).

75. Kielland, K., McFarland, J.W., Ruess, R.W. & Olson, K. Rapid Cycling of Organic Nitrogen in Taiga Forest Ecosystems. *Ecosystems* **10**, 360-368 (2007).

76. Zhang, W.-P. *et al.* Plant litter strengthens positive biodiversity–ecosystem functioning relationships over time. *Trends in Ecology & Evolution* **38**, 473-484 (2023).

77. Gunina, A. & Kuzyakov, Y. Sugars in soil and sweets for microorganisms: Review of origin, content, composition and fate. *Soil Biology and Biochemistry* **90**, 87-100 (2015).

78. Nagar, B.R. Free Monosaccharides in Soil Organic Matter. *Nature* **194**, 896-897 (1962).

79. Takeuchi, T. *et al.* Gut microbial carbohydrate metabolism contributes to insulin resistance. *Nature* **621**, 389-395 (2023).

80. Le Bouguénec, C. & Schouler, C. Sugar metabolism, an additional virulence factor in enterobacteria. *International Journal of Medical Microbiology* **301**, 1-6 (2011).

81. Liddicoat, C. *et al.* Can bacterial indicators of a grassy woodland restoration inform ecosystem assessment and microbiota-mediated human health? *Environment International* **129**, 105-117 (2019).

82. Bulsiewicz, W.J. The Importance of Dietary Fiber for Metabolic Health. *American Journal of Lifestyle Medicine* **17**, 639-648 (2023).

83. Cryan, J.F. *et al.* The Microbiota-Gut-Brain Axis. *Physiological Reviews* **99**, 1877-2013 (2019).

84. Flinders_University. DeepThought (HPC). Retrieved from https://doi.org/10.25957/FLINDERS.HPC.DEEPTHOUGHT. 2021.

85. Pawsey_Supercomputing_Research_Centre. Setonix Supercomputer. Perth, Western Australia; 2023.

86. Langmead, B. & Salzberg, S.L. Fast gapped-read alignment with Bowtie 2. *Nature Methods* **9**, 357-359 (2012).

87. Overbeek, R. *et al.* The SEED and the Rapid Annotation of microbial genomes using Subsystems Technology (RAST). *Nucleic Acids Research* **42**, D206-D214 (2013).

88. Silva, G.G.Z., Green, K.T., Dutilh, B.E. & Edwards, R.A. SUPER-FOCUS: a tool for agile functional analysis of shotgun metagenomic data. *Bioinformatics* **32**, 354-361 (2015).

89. Oksanen, J. *et al.* vegan: Community Ecology Package. R package version 2.5-7.; 2020.